ALEPH 86-43
W. Blum et al.
7.4.1986

Distr.: TPC

MEASUREMENT OF AVALANCHE BROADENING CAUSED BY THE WIRE ExB EFFECT

W. Blum, U. Stiegler, Max-Planck-Institut für Physik, München, FRG
P. Gondolo, L. Rolandi, University of Trieste and INFN, Italy

Abstract

We report measurements of the wire ExB effect in a TPC, the main contribution to its point measuring accuracy. We describe briefly a small TPC with a rotatable wire frame and the method to isolate the effective drift direction $\tan\psi$ of the electrons and the strength g of the effect. Values of $\tan\psi$ and g are shown for various magnetic fields and gas mixtures of Ar and CH_4, obtained with laser- and particle-tracks.

Talk presented at the Vienna Wire Chamber Conference by W. Blum, 26.2.86

In gas chambers every track coordinate measurement along a proportional wire is limited in its precision by the width of the avalanches, because the statistical nature of the ionisation gives rise to fluctuations of the centre position which are proportional to the width of the avalanche. Apart from the negligible intrinsic width related to the internal avalanche mechanism, the two main causes for an increase of the width are the transverse diffusion of the ionisation electrons on their way from the track to the wire and, in the presence of a magnetic field across the wire, the combined electric and magnetic fields near the wire which bend the drift trajectories into the wire direction ("ExB-effect") [1].

The time projection chambers (TPC) presently constructed for the ALEPH and DELPHI experiments at LEP operate at atmospheric gas pressure in contrast to the TPC at PEP operating at 8.5 atm. When reducing the gas pressure and the drift field by a factor η, the fluctuation of the avalanche centre position due to transverse diffusion will remain the same if the magnetic field is kept constant, because the diffusion constant D and the relevant statistical factor both vary as η while the magnetic reduction of D [ref.2] is nearly proportional to $1/\eta^2$. The ExB-effect does not scale, and it cannot be calculated easily because it depends on the unknown details of the scattering cross sections at high field strengths. Both the angle of deviation and the statistical factor are worse at low pressure, so that we had to measure them for the ALEPH TPC, using a small model with the same electrode configuration inside a magnet. Before we describe the apparatus in detail we want to explain why it has a rotatable wire frame.

Method

For a track parallel to the pad axis, the point measuring accuracy σ_m depends on the angle α between the track and the wire normal (Fig. 1) in the following way :

$$\sigma_m^2 = \sigma_o^2 + g^2(\tan\alpha-\tan\psi)^2\cos^2\alpha = \sigma_o^2 + (g^2/\cos^2\psi)\sin^2(\alpha-\psi); \qquad (1)$$

ψ is the effective angle under which the drifting electrons approach the wire, and g^2 represents the variance of the centre position of the ionisation.The quantity g^2 depends on the geometry of the wire chamber (pad length, distance between sense wires) and on the ionisation mechanism, i.e. the density of primary ionisation clusters and the number of electrons in the clusters. This dependence will be elaborated further down. σ_o, finally, stands for all the other contributions to the point measuring accuracy which are independent of α like diffusion or electronics errors.

The method is to determine σ_m^2 for every condition as a function of the angle α and to determine the three parameters σ_o, g and ψ from a least-squares fit to this function. The best way to vary α consists of a variation of the wire orientation so that the angle between the pads and the track remains unchanged. If, instead, the wires are fixed to the pads then a variation of α changes the angle between tracks and pads, introducing uncontrollable errors through the rapidly changing pad response function, especially when the pads are as long as they are here (3 cm).

Apparatus [3]

For this reason the wire frame is rotatable and circular in shape resulting in a cylindrical construction which is mounted on the horizontal cathode plate segmented as the ALEPH cathode plate but with only 4 straight pad rows (Fig. 2). The pad pulses are fed into the ALEPH preamplifiers, are then shaped and digitized by integrating ADC's. There are no amplifiers on the wires. The signal wires and the field wires are connected to one common voltage source each; the upper grid, rotating with the sense-and-field-wire grid, is electrically connected to the cathode plate (ground). The gas volume is closed by a cylindrical cover 10 cm high with diameter 40 cm which has two quartz windows for the passage of a central laser beam 4 cm above the wires. The cover is also the field cage with the plane electrode opposite the wires, and rings with a graded potential on the mantle inside. The wire frame can be rotated from outside the chamber by two strips to be pulled; the angular position is signaled with the help of suitable contacts inside.

The laser beam was derived from a pulsed MOPA400 N_2-laser, 5 m away from the chamber. An aperture with a 2 mm diameter was placed 3.8 m downstream of the source. The wave length was 330 nm, the pulse length 0.5 ns, the frequency 3 Hz, the integrated power typically 100 µJ. The gas was a mixture of "pure" Argon and "pure" Methane which nonetheless was easily ionised by the light beam. Weak grey filters were used to adjust the ionisation to the level of approximately a minimum-ionising particle.

The particle beam in the CERN SPS was adjusted for 50 GeV pions. The particles incident on the chamber were decay-muons behind 1.2 m of iron. The flux was several muons per burst on a sensitive area of 4x4 cm in the centre of the chamber.

Measurements

We began with laser tracks. For every condition we took 400 shots at each of 9 or more angles α and at positive and negative magnetic field. For each shot, a straight line fit was made through the 4 coordinates y_i^k (k = 1,400) derived from the pad signals, this derivation was based on the known Gaussian shape of the pad response function. One half of the sum of the squared residuals was one measurement of the point measuring accuracy σ_p^2.

We satisfied ourselves that the residuals of a straight line fit through the 4 averages $y_i = \frac{1}{400} \Sigma\, y_i^k$ were small, typically between 0 and $(30\ \mu m)^2$. This shows that the systematic errors were small in comparison to the statistical errors, they were always subtracted from the σ_p^2.

The frequency distribution of the 400 values of σ_p^2 obtained in this way was similar to a scaled χ^2-distribution with 2 degrees of freedom and a tail. An (iterative) cut was applied at 4.5 times the mean value, eliminating between 3% and 5% of the data. The average of the remaining values of σ_p^2 is σ_m^2, the point measuring accuracy for the given angle α.

The curves in Fig. 3 are examples of the variation of σ_m with α. The 3 parameters g, ψ and σ_o were then fitted to equ. (1). Their errors were scaled so that the χ^2 corresponded to the appropriate number of degrees of freedom. The r.m.s. errors of the σ_m^2 were found to be 0.10 of σ_m^2.

We took measurements with various drift fields and a number of sense wire voltages (U_S between 1300 and 1850 V) where the field wire voltage was adjusted for constant gain. Both these variations had essentially no effect on g, ψ and σ_o. Mostly the running conditions were near U_S = 1300 V, U_F = 0, depending on the laser intensity and the gas.

We also varied the gas composition and the magnetic field. Finally, particles were used in place of the laser tracks.

Results

The value of g obtained from the laser tracks depends on the laser beam properties. These were adjusted so that g fell mostly into the range between 0.1 and 0.2 mm, near the value obtained for particles. The value of ψ is independent of the nature of the ionisation.

In Fig. 4 we plot the measured dependence of $\tan\psi$ on magnetic field in 80% Ar + 20% CH_4. One notices a proportional behaviour up to the region where $\tan\psi \approx 1$; then, $\tan\psi$ varies less than proportionally. Up to 10 kG the curve fits the relation

$$\tan\psi = (0.076 \pm 0.002)\,kG^{-1} \cdot B\ .$$

Computer Simulation of the Declustering

Primary ionisation points were created along a track over the length of the pads (3 cm). Their number was chosen according to a Poisson distribution around 35 points per cm (corresponding to a very fast particle in pure Ar), their position was chosen at random from a uniform distribution. With each point a number of electrons was associated at random from the distribution of the cluster size. The cluster size distribution was taken from ref.[4] with the modification that the large number N of electrons above N = 15 (3.2% of the cases) was taken from ref.[5] in order to represent exactly the high end of the distribution. For each electron a position in the sense wire plane was chosen according to a Gaussian distribution law which has the variable parameter s. Each electron was subsequently placed onto the nearest sense wire according to a given Lorentz direction $\tan\psi$, representing the ExB effect near the wire. The average of all electron positions in the wire direction was one "coordinate measurement" of the track segment. From a large number of coordinate measurements we determined the r.m.s. width and called it σ, the measurement accuracy of a pad row. In Fig. 6, σ is plotted against s for 3 different Lorentz directions.

The effect of declustering is clearly visible: As the diffusion parameter s increases from zero, the measuring accuracy becomes much better (σ smaller), σ reaches a minimum where s is roughly equal to one half of the wire distance; then σ increases until

$$\sigma = s/\sqrt{N_{tot}} ,$$

equal to the r.m.s. deviation of the centre of N_{tot} electrons after a diffusion s. In this regime, σ is independent of ψ. The curve is meant to show the principle of the declustering effect. Before comparing it to experimental data it would have to be modified according to the pulse height cuts appropriate to the experiment.

The effect is obviously quite interesting for the large TPC's now under construction for DELPHI and ALEPH, because the expected single-electron diffusion after 1 m (2 m) of drift is roughly 1.0 mm (1.4 mm), close to the minimum σ.

Conclusion

The wire ExB effect can be isolated very well with a TPC which has a rotating wire frame. The measurements show a strong dependence on the gas composition which needs to be understood.

We also discovered a substantial reduction of the wire ExB effect through "declustering" caused by diffusion. A Monte-Carlo simulation supports the observation.

We show in Fig. 5 the measured dependence of $\tan\psi$ on the Methane concentration in our gas mixture of Ar and CH_4. There is a clear trend for $\tan\psi$ to be larger for higher CH_4 content but this trend does not continue below 10%. The values of $\tan\psi$ are averages over several independent measurements at 15 and 17 kG; the curve in Fig. 4 was used to reduce them to their value at 15 kG. Our value at 10% Methane is $\tan\psi = 0.69\pm0.03$, it may be compared to the result of Amendolia et al. [1] which was $\psi = (29\pm3)°$; both are in agreement within 2 standard deviations.

The most interesting result was obtained with particles, especially from a comparison of the data with and without magnetic field, see table 1. Keeping in mind that a magnetic field of 15 kG reduces the transverse diffusion coefficient by a factor of 50 [2] we expect for the mean square width of the diffusion cloud after 4 cm of drift a value of 1.6 mm^2 (B = 0) or $3.2\times10^{-2} mm^2$ (B = 15 kG). Since on the pad length of 3 cm the number of ionisation electrons is approximately 300, the expected change in the uncertainty of the centre is $\sigma_o^2(B = 15) = 0.5\times10^{-2} mm^2$, equal to the measured difference appearing in table 1. - The reduction of the value of g^2 by a factor of 3 is attributed to the increase in diffusion. We propose that the mechanism responsible for this reduction is the declustering of the original ionisation by diffusion: Immediately after the passage of the high-energy particle, the electrons exist in clusters of between 1 and sometimes a large number of them. When the charge centre of a segment of track is measured electronically it will fluctuate around its true position according to the small number of clusters and their variation in size. If, however, the electrons suffer diffusion on their way to the wires the space correlation due to the clustering is broken, either completely or to some extent, depending on the diffusion. In the limit that the diffusion is large compared to the wire distance, the charge centre of a segment of track will fluctuate only according to the total, larger, number of electrons. In our experiment the distance between sense- and field-wires was 2 mm and the diffusion at B = 0 comparable, whereas at B = 15 kG, the diffusion was small compared to the wire distance. It is the matter of a detailed calculation to know how big a diffusion is needed to break the correlation before the sheer size of the diffusion cloud dominates the fluctuation.

Laser tracks do not show this behaviour, see table 2. Here the value for g^2 is the same (within 2½ standard deviations) for B = 0 and B = 17 kG. The ionisation intensity must have been the same within, say, ±10% although it was not especially monitored.

Table 1

Values of σ_o^2, g^2 and ψ measured with and without magnetic field in 90%Ar + 10%CH_4 using high-energy particles.

B(kGauss)	$\sigma_o^2(10^{-2}mm^2)$	$g^2(10^{-2}mm^2)$	ψ(deg)
15	1.08±0.03	4.8±0.1	32.3±1.5
0	1.58±0.06	1.6±0.15	-1±2

Table 2

Values of σ_o^2, g^2 and ψ measured with and without magnetic field in 90%Ar + 10%CH_4 using a laser beam.

B(kGauss)	$\sigma_o^2(10^{-2}mm^2)$	$g^2(10^{-2}mm^2)$	ψ(deg)
17	2.0±0.1	2.5±0.2	51±1.5
0	3.1±0.1	3.02±0.05	1±5.5

References and Footnotes

[1] C.K. Hargrove et al., N.I.M. 219, 461 (1984)
S.R. Amendolia et al., N.I.M. 219, 461 (1984).

[2] S.R. Amendolia et al., N.I.M. A244, (1986). 516.

[3] A more detailed description of the apparatus as well as a list of measurement results are contained in : U. Stiegler; "Die Ortssuflösung der Spuren-driftkammer im Magnetfeld, Diplomarbeit Universität München, 1985 (unpublished), available at the MPI Munich (MPI-PAE/Exp. El.159, January 1986).

[4] F. Lapique and F. Piuz, N.I.M. 175, 297 (1980).

[5] V.C. Ermilova, N.I.M. 145, 555 (1977).

Figure Captions

Fig. 1 Definition of the angles α and ψ in the wire plane.

Fig. 2 Arrangement of the electrodes.
All the wires are mounted on the one rotatable frame.

Fig. 3 Examples of the measured accuarcy squared, σ^2, versus the angle α between track and wire-normal, for positive and negative B-field. The curves are fits to expression (1).

Fig. 4 Measured dependence of $\tan\psi$ on magnetic field in 80% Ar + 20% CH_4.

Fig. 5 Measured dependence of $\tan\psi$ on the methane concentration.

Fig. 6 Calculated dependence of the point measuring accuracy σ on the diffusion parameter s. To the left, σ is dominated by the wire ExB effect, to the right by diffusion; in between, the diffusion reduces the wire ExB effect. 3 different ψ.

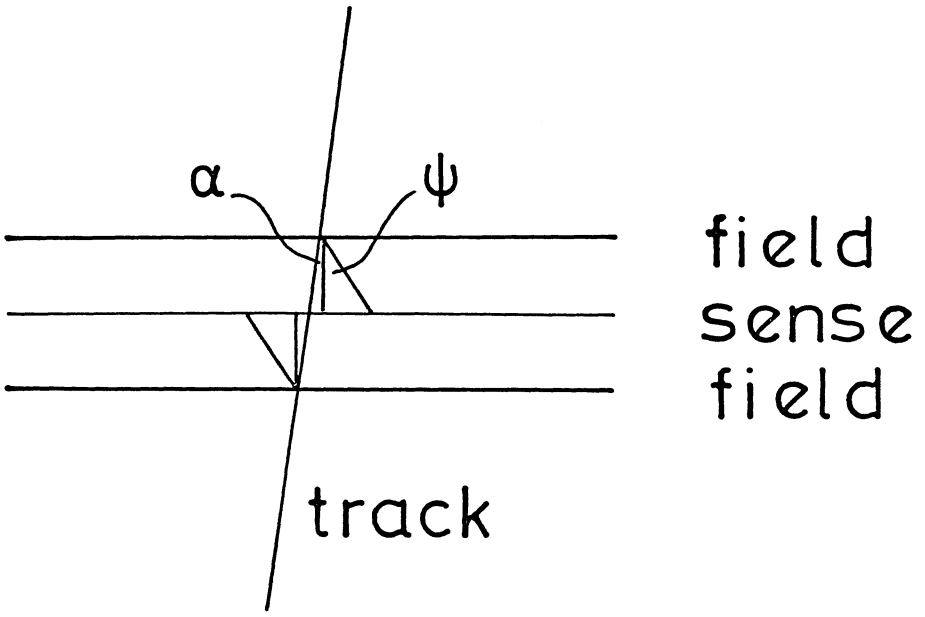

Fig. 1

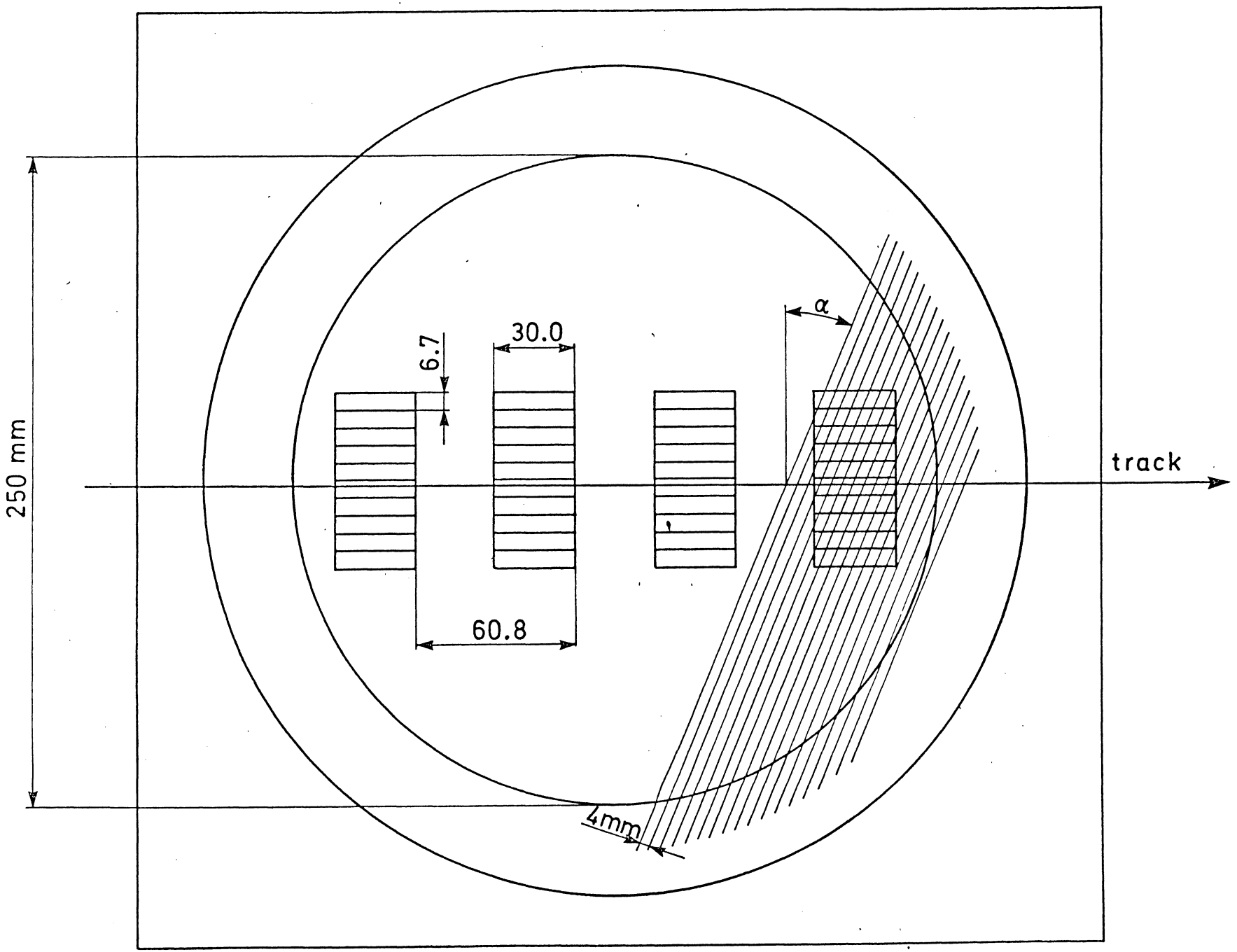

Fig 2a

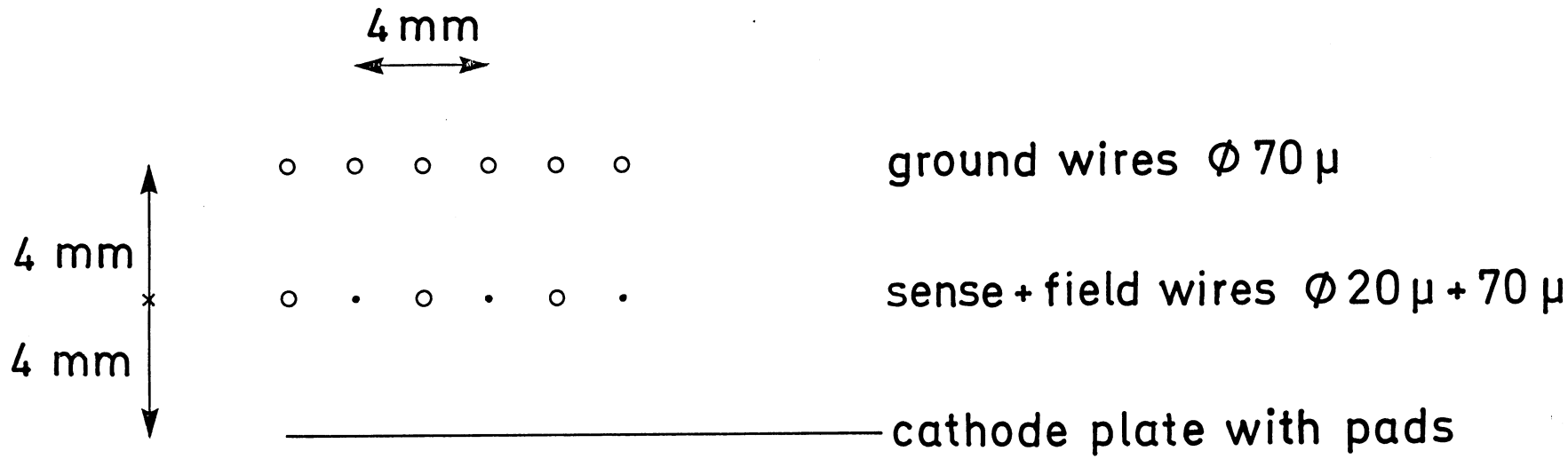
4 mm
4 mm
4 mm
ground wires Ø 70 µ
sense + field wires Ø 20 µ + 70 µ
cathode plate with pads

Fig 2b

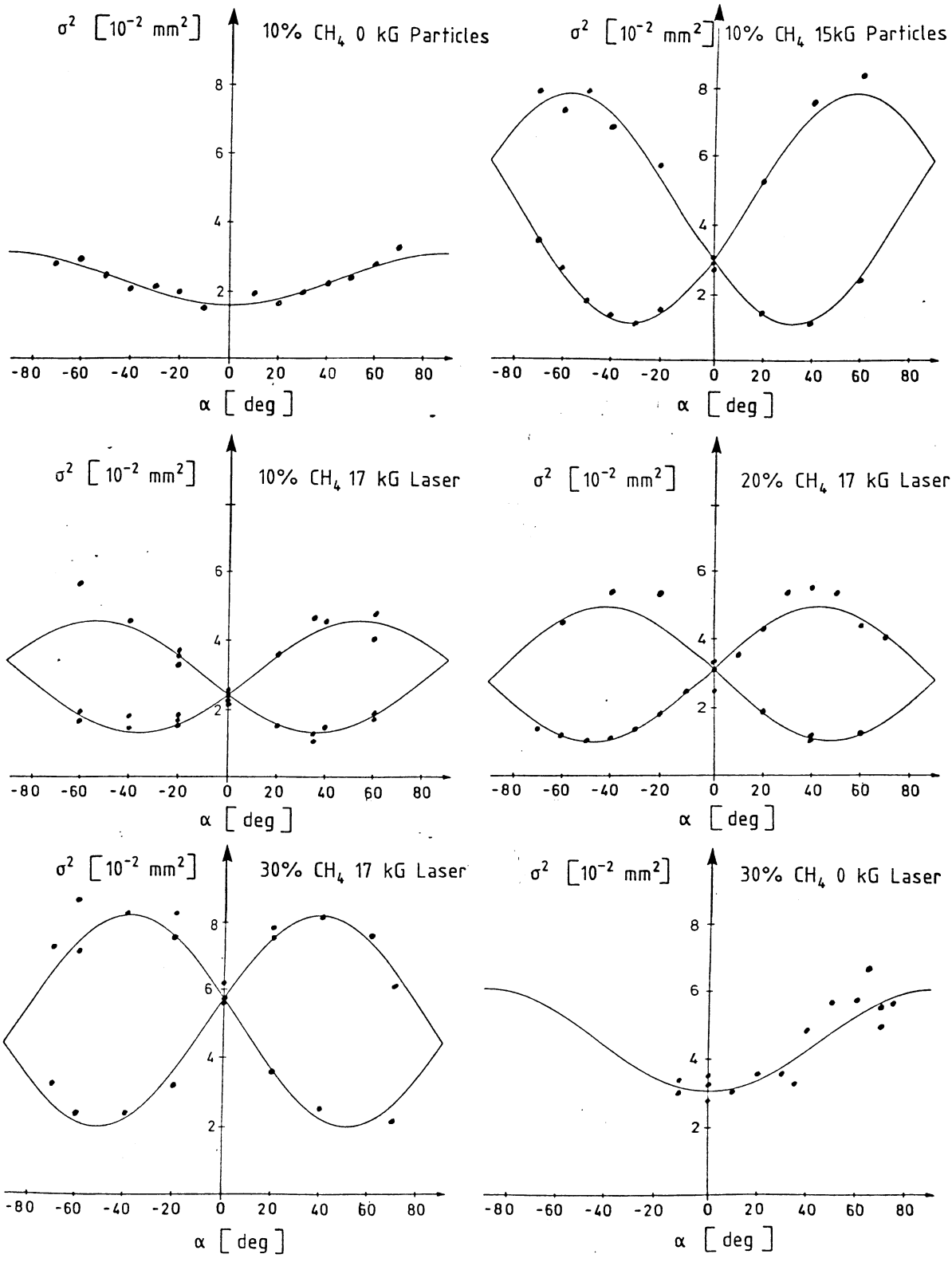
σ² [10⁻² mm²]
10% CH₄ 0 kG Particles
σ² [10⁻² mm²]
10% CH₄ 15kG Particles
σ² [10⁻² mm²]
10% CH₄ 17 kG Laser
σ² [10⁻² mm²]
20% CH₄ 17 kG Laser
σ² [10⁻² mm²]
30% CH₄ 17 kG Laser
σ² [10⁻² mm²]
30% CH₄ 0 kG Laser
α [deg]
-80 -60 -40 -20 0 20 40 60 80
2 4 6 8

Fig. 3

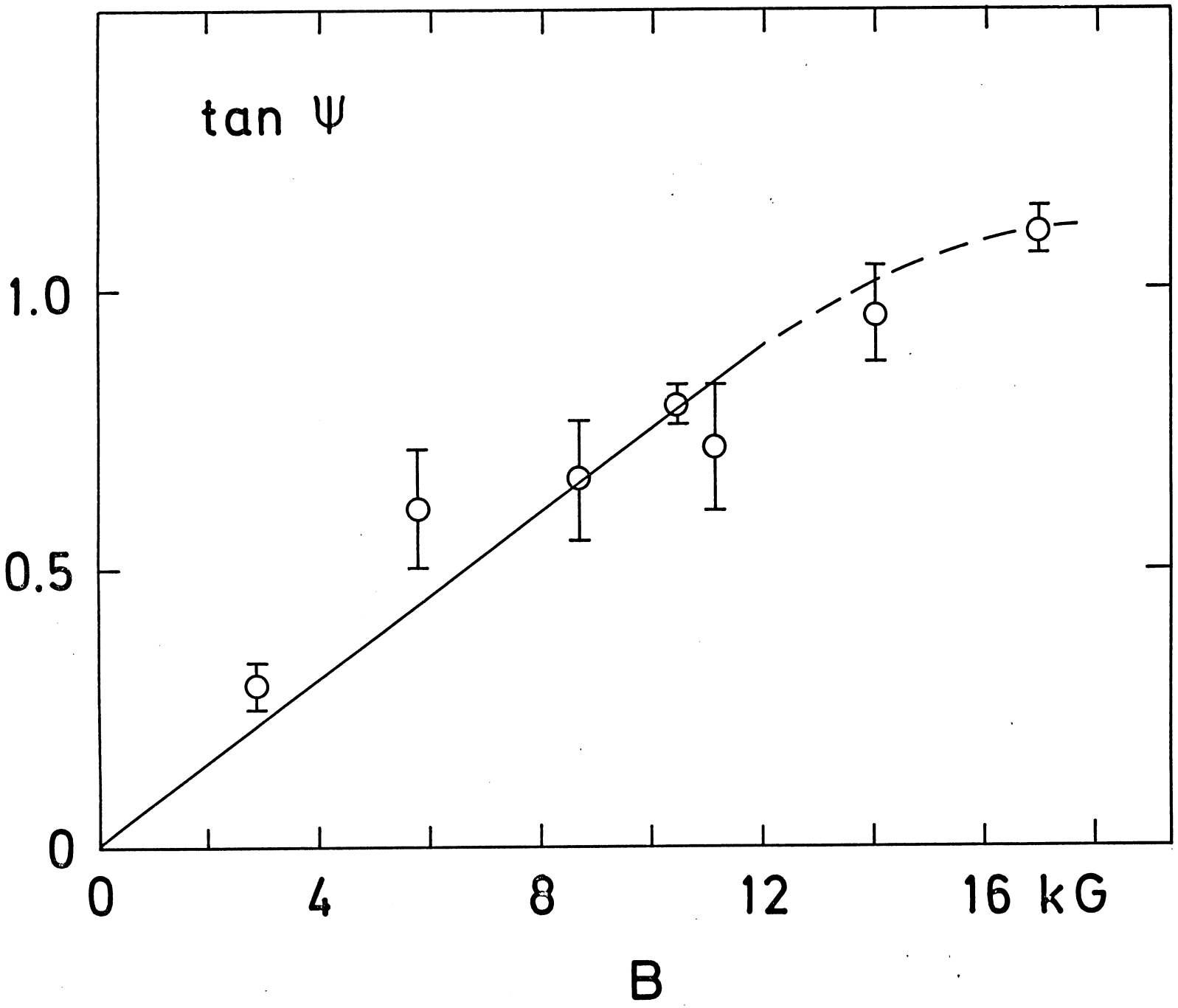

Fig. 4

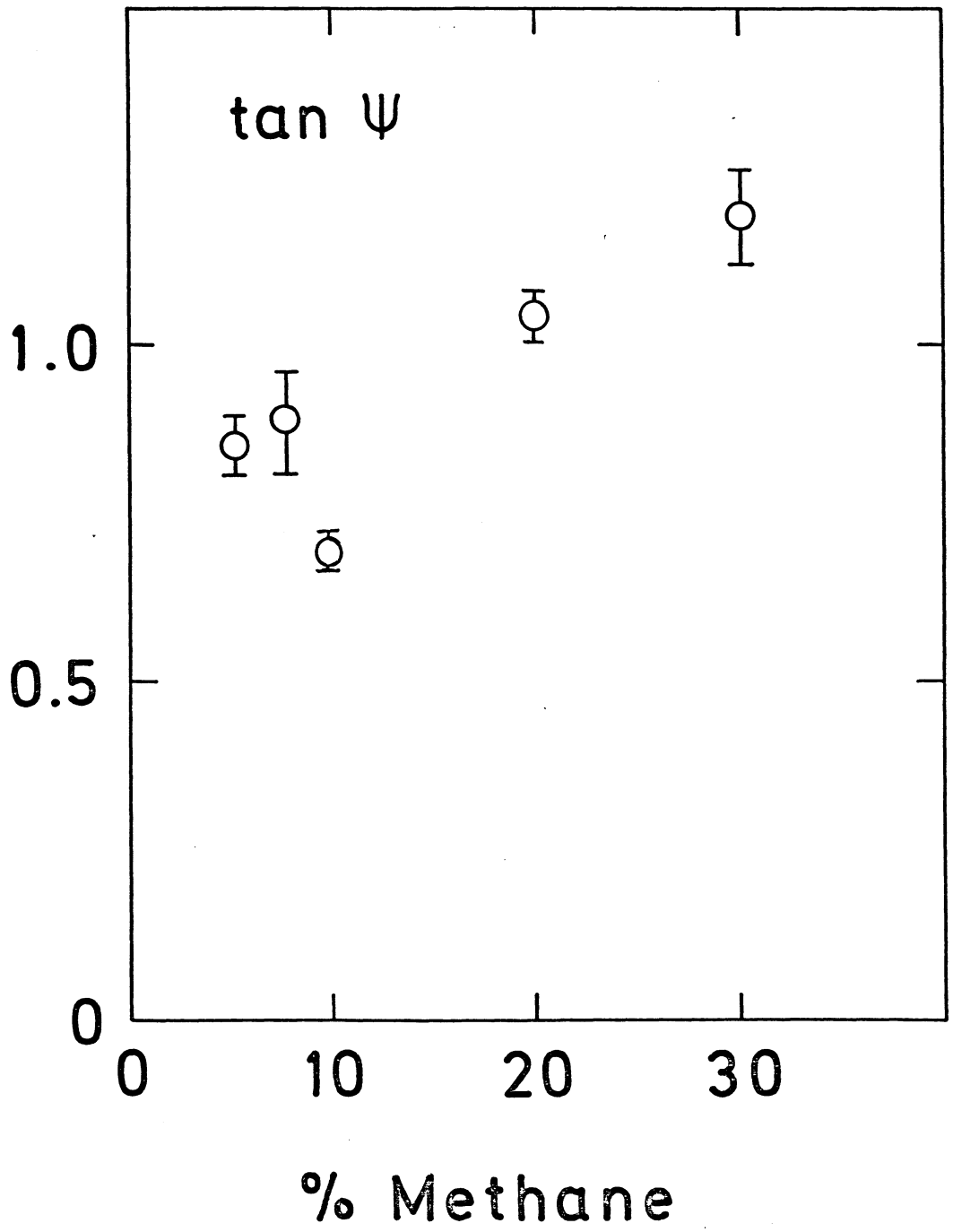

Fig 5

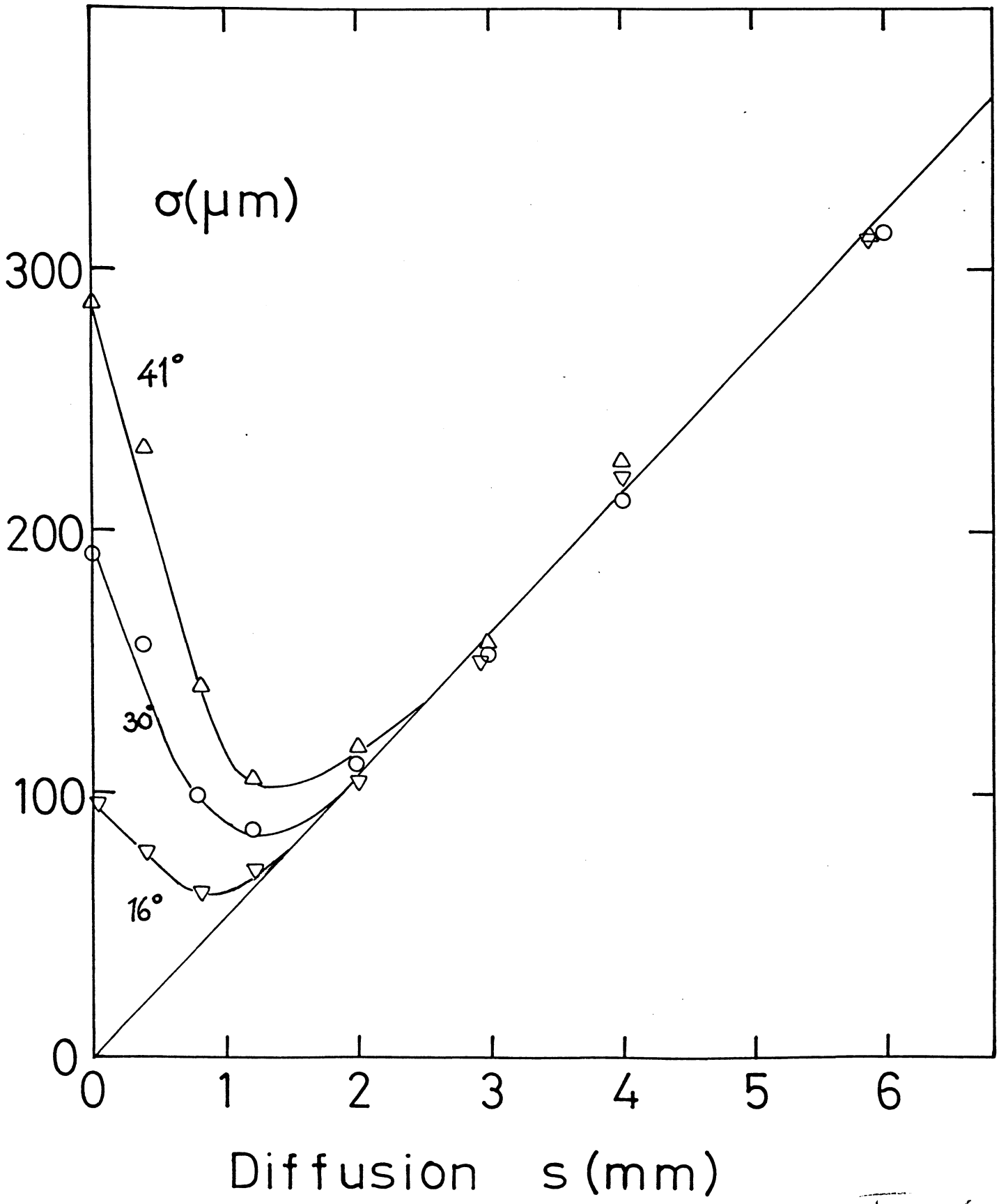

Fig. 6